

One polymer with three charge states for two types of lithium-ion batteries with different characteristics as needed[☆]

Yang Zhao^{a,c}, Manman Wu^{a,c}, Hongtao Zhang^{a,c}, Zhen Ge^{a,c}, Chenxi Li^{a,c}, Yanfeng Ma^{a,c}, Yongsheng Chen^{a,b,c,*}

^a The Centre of Nanoscale Science and Technology and Key Laboratory of Functional Polymer Materials, Institute of Polymer Chemistry, College of Chemistry, Nankai University, Tianjin 300071, China

^b State Key Laboratory of Elemento-Organic Chemistry, Nankai University, Tianjin, 300071, China

^c Renewable Energy Conversion and Storage Center (RECAST), Nankai University, Tianjin 300071, China

ARTICLE INFO

Keywords:

Lithium-ion batteries
organic electrodes
three charge states
two types of batteries
high-performance

ABSTRACT

Organic batteries materials exhibit merits of diverse structures, high capacities, less pollution and abundant sources, therefore, developing high-performance organic electrode materials is promising for the next generation of rechargeable batteries. Various advanced organic cathode materials have been reported but most of them possess only two charge states and can be used for one kind of battery. Thus, it is challenging to design organic material with three charge states for two types of high-performance organic batteries with different characteristics as needed. Herein, we designed and synthesized a polymer named P-BQPZ, which integrates maximum n-type and p-type redox-active moieties into one stable polymer with minimum redox-inactive moieties, and thus it can be used for two types of long-life lithium-ion batteries with different features (e.g. high capacity or output potential) by using different redox-active sites. The cathode half-cell based on n-type redox-active reaction exhibits a high capacity of 431.3 mA h g⁻¹ (2.4 V vs Li/Li⁺) at 50 mA g⁻¹ and a high retention of 99.95% per cycle up to 500 cycles at 1,000 mA g⁻¹. Furthermore, the cathode half-cell based on p-type redox-active reaction displays relatively high output voltage of 3.1 V (vs Li/Li⁺, 176.6 mA h g⁻¹ at 50 mA g⁻¹) and superior retention of 99.97% per cycle at 500 mA g⁻¹ for 1,000 cycles. More importantly, two kinds of all-organic batteries by using P-BQPZ cathode also operate well.

1. Introduction

Lithium-ion batteries (LIBs) have attracted much interests as the dominant energy storage systems [1–4]. Most traditional and commercial LIBs have been using inorganic electrode materials, which face challenges of scarce sources, toxicity, environmental pollutions and low specific capacities [5–9]. Therefore, it is essential to find alternative electrode materials for the increasing energy demands of the society and human beings. Compared to inorganic electrode materials, organic electrode materials are naturally abundant, nontoxic and environmentally friendly, which makes them promising for the large-scale utilization of LIBs in the future. More importantly, organic materials exhibit highly designable structures and light atomic weights, likely leading to tunable functions and high specific capacities [10–13].

Normally, organic electrode materials can be categorized into three types based on the redox reactions: n-, p- and bipolar-type [14,15]. N-type materials intend to be reduced from their neutral state and result in

negatively charged states, such as those containing C = O, C = C and S-S groups [14,15]. P-type materials typically intend to be oxidized from their neutral states and lead to positively charged states, such as triphenylamine derivatives and conductive polymers containing -NH groups [16,17]. These two types of materials generally containing only one type of redox pair and thus could be used for one type of battery. But bipolar-type materials could possess both n-type and p-type redox reactions, which then could generate two redox pairs, such as those containing organic radicals [14,18]. Therefore, two types of organic batteries by using the same bipolar starting material could be designed and fabricated.

So far most reported advanced organic cathode materials could exhibit only n-type or p-type redox reactions with two charge states including neutral state and one charged state (positively or negatively charged states) [19]. However, it's a great challenge and has not been reported to design and obtain an organic cathode material which possesses three charge states and be used for two kinds of LIBs with different characteristics. With this material, different batteries having different performances might be chosen and applied as required.

[☆] Dedicated to the 100th anniversary of Chemistry at Nankai University

* Corresponding author at: Nankai Univ, Weijin Rd 94, The Ins of Polymer Chemistry Colleg, Tianjin, Tianjin 300071, China.

E-mail address: yschen99@nankai.edu.cn (Y. Chen).

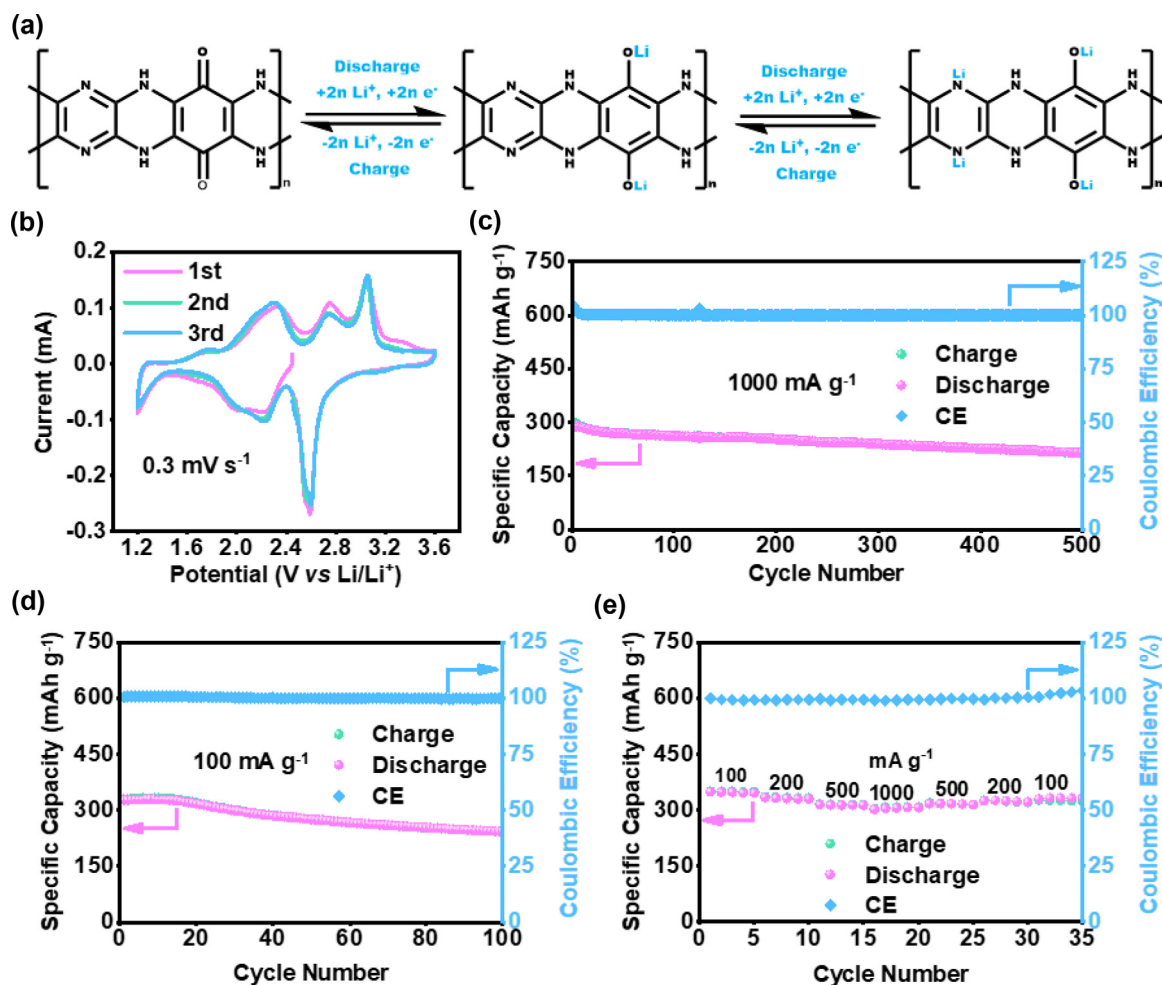


Fig. 2. Electrochemical performance of the cathode half-cell based on n-type redox reaction of P-BQPZ between 1.2 and 3.6 V (vs Li/Li^+). (a) Lithiation/delithiation processes of P-BQPZ. (b) Cyclic voltammetry (CV) curves for consecutive three cycles at 0.3 mV s^{-1} . (c) Cycling performance at a current of 1000 mA g^{-1} for 500 cycles. (d) Cycling performance at a current of 100 mA g^{-1} for 100 cycles. (e) Rate performance at current densities of 100, 200, 500 and 1000 mA g^{-1} after activation under 50 mA g^{-1} .

Herein, we proposed a strategy that integrates multiple n-type and p-type redox-active groups into one stable polymer with minimum redox-inactive groups (to maximize capacity) to obtain a bipolar organic cathode material with three charge states, which could be used for two types of LIBs with high performances and different features (Scheme 1) [20,21]. In previous reports, many n-type electrode materials containing C = O or C = N groups can afford fast reaction kinetics and high specific capacities [15]. P-type organic electrode materials, such as polyaniline and its derivations possessing -NH redox-active groups, can exhibit good cycling stability and high redox potentials over 3.0 V (vs Li/Li^+) [22–26]. Ladder polymers show good thermal and electrochemical stability, which have been used for many organic batteries with long cycle life [27,28]. So, it is believed that by integrating plenty of redox-active C = O, C = N groups (n-type moieties) and -NH linkages (p-type moieties) into one ladder polymer, a stable polymer possessing three charge states could be obtained and used for two different high-performance LIBs.

Thus, a novel polymer named P-BQPZ that contains maximum redox-active moieties of both n-type and p-type and minimum redox-inactive groups is designed and synthesized through a simple one-step condensation reaction between two commercial monomers named 2,3,5,6-tetramino-1,4-benzoquinone (TABQ) and 2,3,5,6-tetrachloro-pyrazine (TCPZ). Two types of high-performance organic LIBs with different characteristics can be assembled by utilizing its n-type or p-type redox-active moieties in different potential ranges, respectively. Specifically, when n-

type moieties (C = O and C = N groups) are used as redox-active sites, the cathode half-cell exhibits theoretical and experimental capacities as high as 446.7 and $431.3 \text{ mA h g}^{-1}$ (at 50 mA g^{-1} , 2.4 V vs Li/Li^+), respectively, which are higher than many previously reported organic cathode materials (Fig. S8, Table S2). In addition, it displays good cycling stability with a high retention of 99.95% per cycle up to 500 cycles at 1000 mA g^{-1} . On the other hand, when p-type moieties (-NH groups) are used as the redox-active centers, the cathode half-cell not only exhibits a higher working potential of $\sim 3.1 \text{ V}$ (vs Li/Li^+) with a capacity of $176.6 \text{ mA h g}^{-1}$ (at 50 mA g^{-1}) but also an excellent cycling stability with retention of 99.97% per cycle up to 1000 cycles (at 500 mA g^{-1}). In general, P-BQPZ with three charge states and two pairs of redox reactions can be used to build two long-life organic LIBs with either high capacity or high working potential, which could be taken as needed for practical requirements (Table 1). Furthermore, two types of all-organic batteries based on P-BQPZ cathode are also assembled, and both of them operate well in their voltage windows. Such one starting material, which can be used as cathode material to fabricate two different high-performance organic batteries, has not been reported so far. These results and our strategy thus could offer a promising approach to design better organic batteries materials with even higher performance to fully capitalize the potential of next generation of rechargeable batteries based on organic materials.

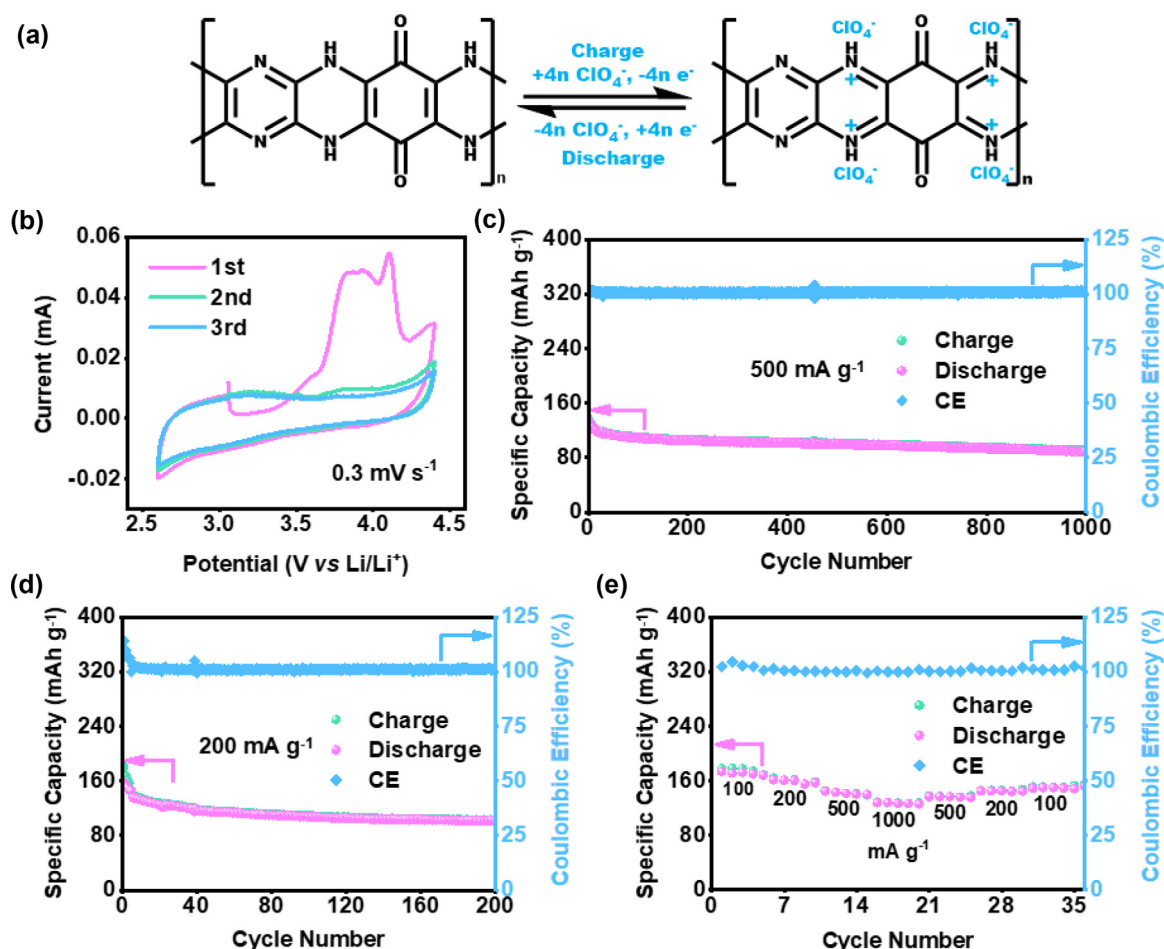


Fig. 3. Electrochemical performance of the cathode half-cell based on p-type redox reaction of P-BQPZ between 2.6 and 4.4 V (vs Li/Li⁺). (a) P-type redox behavior of P-BQPZ. (b) CV curves for consecutive three cycles at 0.3 mV s⁻¹. (c) Cycling performance at a current of 500 mA g⁻¹ for 1000 cycles. (d) Cycling performance at a current of 200 mA g⁻¹ for 200 cycles. (e) Rate performance at current densities of 100, 200, 500 and 1000 mA g⁻¹ after activation under 50 mA g⁻¹.

Table 1

Comparison of the two types of batteries based on n-type or p-type redox reactions of P-BQPZ.

Reaction type	Redox States	Counter Ion	Capacity (50 mA g ⁻¹)	Working Potential
N-type	Neutral and negatively charged states	Li ⁺	431.3 mA h g ⁻¹	2.4 V (vs Li/Li ⁺)
P-type	Neutral and positively charged states	ClO ₄ ⁻	176.6 mA h g ⁻¹	3.1 V (vs Li/Li ⁺)

2. Results and discussion

P-BQPZ was obtained by the polymerization reaction between TCPZ and TABQ, of which three different carbon atoms exist (Fig. 1a). TGA result shows that only very minor mass loss up to 300 °C under nitrogen condition, indicating good thermal stability of P-BQPZ (Fig. 1b). Fig. 1c gives the ¹³C solid state NMR spectrum of P-BQPZ, of which the peaks at 174.6, 146.0 and 130.2 ppm match well with the desired structure where three different carbon atoms exist (labels in blue of Fig. 1a and 1c) [29,30]. This is also supported with the observed peaks of C 1 s, N 1 s, O 1 s and Cl 2p in the XPS survey spectrum (Fig. 1d) [20,31,32]. The FT-IR analysis reveals the existence of C = O (1623 cm⁻¹), C = N (1538 cm⁻¹) and -NH (3460 cm⁻¹) redox-active groups in the structure of P-BQPZ (Fig. 1e) [20,30,33]. Peak of -NH₂ bonds (3156 cm⁻¹) and peak of -C-Cl bonds (653 cm⁻¹) from the starting monomers TABQ and TCPZ, respectively, almost disappear completely after polymerization, indicating complete consumption of the monomers during the polymerization process [34]. In its Raman spectrum, P-BQPZ displays a typical D band (1387 cm⁻¹) and G (1517 cm⁻¹) band, which is similar with graphene and its derivatives (Fig. S3) [35]. P-BQPZ shows a BET surface area of

43.1486 m² g⁻¹ with an average pore width of 5.58 nm (Fig. S4). From its FE-SEM and EDS images (Fig. S5), P-BQPZ possesses uniform morphology and elemental distribution. These results indicate that we successfully synthesized P-BQPZ with the expected multiple redox-active groups and stable polymer backbone.

With this bipolar material in hand, its electrochemical performances as cathode material were carried out systematically. In the potential range of 1.2–3.6 V (vs Li/Li⁺), its n-type redox-active moieties (C = O and C = N groups) can reversibly be reduced and combine with Li⁺, and P-BQPZ reversibly transform from its neutral state to negatively charged state (Fig. 2a). Its high theoretical capacity (446.7 mA h g⁻¹) is confirmed with the experimental result (431.3 mA h g⁻¹ at 50 mA g⁻¹), which is among the best previous reports (Fig. S7, S8 and Table S2). Its reversible redox reaction is confirmed by CV curves (Fig. 2b), which show clear and reversible redox peaks of n-type redox reactions of P-BQPZ. Redox peaks at 2.6, 2.7 and 3.0 V (vs Li/Li⁺) can be assigned to the redox reaction of the C = O bonds, redox peaks at 2.3 and 2.2 V (vs Li/Li⁺) can be attributed to the C = N bonds [30]. The cathode half-cell based on n-type reaction displays working potential of 2.4 V (vs Li/Li⁺), of which most capacity contribution is obtained in the potential range

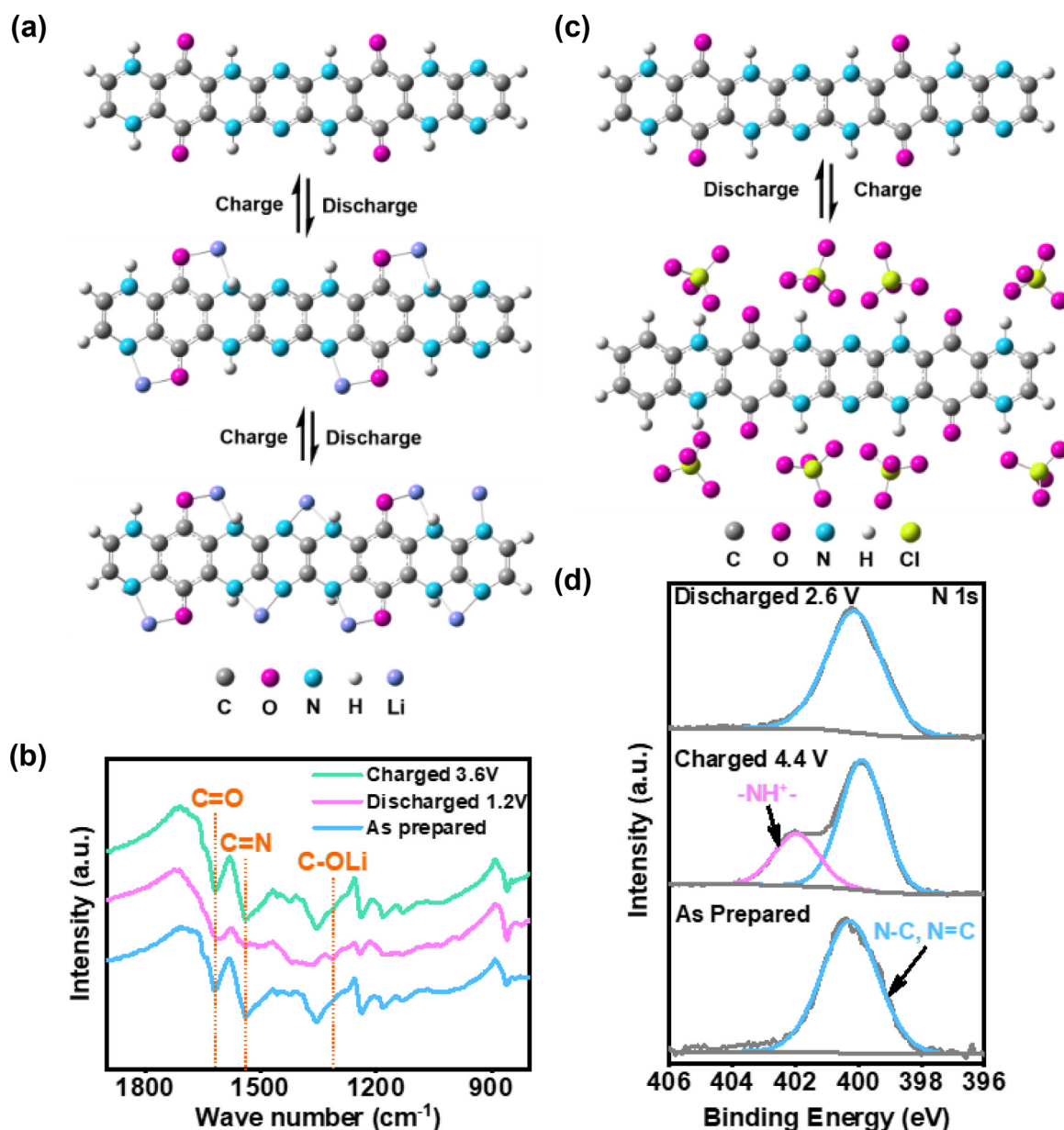


Fig. 4. Redox mechanisms of two types of cathode half-cells made of P-BQPZ. (a) The schematic diagram of the lithiation/delithiation processes based on n-type redox reaction after geometry optimization by the DFT calculations. (b) *Ex situ* IR spectra at different lithiation/delithiation stages collected during the first cycle between 1.2 and 3.6 V (vs Li/Li⁺). (c) The schematic diagram of structural changes during charge/discharge processes based on p-type redox reaction by the DFT optimization. (d) *Ex situ* high-resolution N 1 s spectra at different charge/discharge stages collected during the first cycle between 2.6 and 4.4 V (vs Li/Li⁺).

of 1.2–2.6 V (vs Li/Li⁺). A high reversible capacity of 213.3 mA h g⁻¹ can be retained after 500 cycles under current of 1000 mA g⁻¹ with a high retention of 99.95% per cycle (Fig. 2c). A high reversible discharge capacity can be observed under a current of 100 mA g⁻¹ (Fig. 2d). Superior reversible capacities of 348.4, 333.0, 314.0 and 305.2 mA h g⁻¹ can be obtained under current densities of 100, 200, 500 and 1000 mA g⁻¹, respectively, which presents excellent rate performance (Fig. 2e).

The electrochemical performance of the cathode half-cell based on p-type redox reaction of P-BQPZ in the potential window of 2.6–4.4 V (vs Li/Li⁺) was also studied. -NH groups of P-BQPZ can be oxidized when charged, along with the formation of -NH⁺ bonds and the combination with ClO₄⁻ from the electrolyte, during which P-BQPZ can transform from its neutral state to positively charged state (Fig. 3a) [36,37]. It gives higher working potential of 3.1 V (vs Li/Li⁺) with a capacity of 176.6 mA h g⁻¹ at 50 mA g⁻¹ (Fig. S11). A high retention of 99.97% per cycle after 1000 cycles under 500 mA g⁻¹ can be achieved, which

reveals good cycling stability (Fig. 3c). The cathode half-cell based on p-type redox reaction also displays good rate performance, and only subtle capacity decay can be observed when increasing current densities (Fig. 3e). The first cycle of the CV curves of the cathode half-cell based on p-type redox reaction displays irreversible redox peaks, corresponding to the irreversible side reactions of the electrolyte, which is common in polyaniline-based electrode materials (Fig. 3b) [38,39]. It shows comprehensively high potential and capacity among the p-type organic cathode materials for LIBs (Fig. S11, Table S3).

The proposed two-step redox processes of its n-type redox reaction in the potential range of 1.2–3.6 V (vs Li/Li⁺) and DFT calculation results were shown in Fig. 4a [20,40,41]. The calculations were conducted on the two repeating units of P-BQPZ, and two-step two-electron transfer processes can be confirmed. The first four Li⁺ are combined by four O atoms of C = O groups and the adjacent four N atoms of N-H groups, forming four five-member rings (C-O-Li-N-C) [20,30]. Then the reduc-

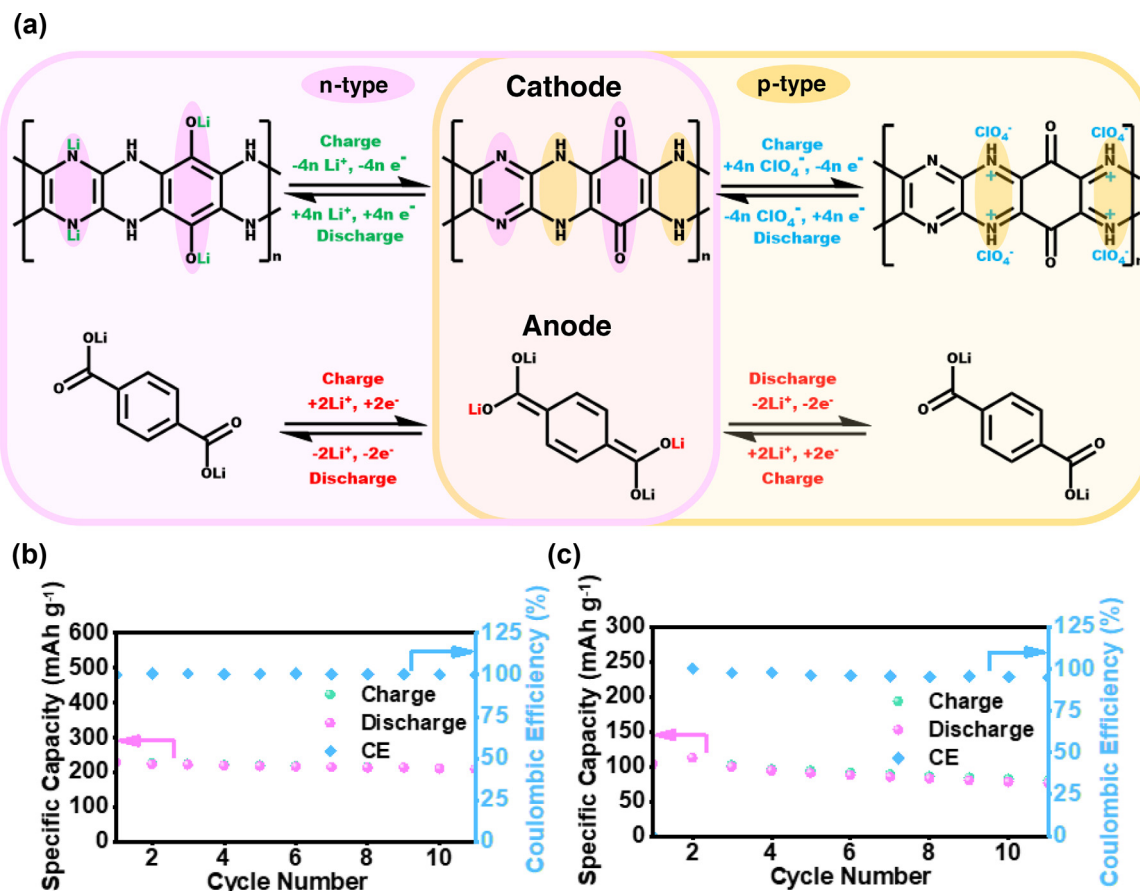


Fig. 5. All-organic batteries based on P-BQPZ cathode with three charge states and Li₂TP anode. (a) Two types of redox processes of the all-organic batteries based on n-type and p-type redox reactions of P-BQPZ, respectively. (b) Cycling performance of the full cell based on n-type redox reaction of P-BQPZ at current of 500 mA g⁻¹ between 0.1 and 2.7 V. (c) Cycling performance of the full cell based on p-type redox reaction of P-BQPZ at current of 50 mA g⁻¹ between 0.1 and 3.4 V.

tion reaction take place on C = N bonds with Li⁺ combined by four N atoms of C = N groups and another four N atoms from N-H bonds nearby [42]. Two repeating units of P-BQPZ could keep its planer structure after insertion of 8 Li⁺ (Figure S14a). The sum of the electronic and thermal free energies of these three states are -1803.181641, -1833.544773 and -1863.621835 Hartree, respectively, and the energy changes of these two lithiation processes are negative, which suggests the spontaneous features of the two-step lithiation processes. To confirm the mechanism of the n-type redox reaction of P-BQPZ, *ex situ* IR tests were conducted to study the changes of chemical bonds during discharge/charge processes (Fig. 4b). Peaks of C = O (1618 cm⁻¹) and C = N (1539 cm⁻¹) bonds become weaker when discharged to 1.2 V (vs Li/Li⁺), and the peak of C-OLi bonds at 1313 cm⁻¹ emerges at the same time, which reveals that the reduction of C = O and C = N bonds [31,43]. When charged to 3.6 V (vs Li/Li⁺), the peak of C-OLi bonds disappears, and the peaks of C = O and C = N groups recover, which shows good reversibility of the cathode half-cell based on n-type redox reaction. We further conducted *ex situ* XPS experiments to verify these redox processes (Fig. S13). It can be seen that peaks of O-Li and N-Li bonds appear after discharging and disappear after charging [44], along with the strengthening and weakening of the peak of Li 1 s, respectively. This means that the intercalation/de-intercalation of Li⁺ into/from the C = O and C = N bonds happen during the n-type discharge/charge processes.

For p-type redox reaction mechanism, we also optimized the structure of the two repeating units of P-BQPZ during the redox process in the potential window of 2.6–4.4 V (vs Li/Li⁺) by DFT calculations (Fig. 4c). The results show that ClO₄⁻ anions from the electrolyte exist near the -NH⁺ bonds when the P-BQPZ is oxidized. The molecular backbone keeps its planer structure, which shows little structural changes

and thus improved stability during the charge/discharge processes (Fig. S14b) [45]. We also conducted *ex situ* XPS tests to confirm the reaction process of the cathode half-cell based on p-type redox reaction. The high-resolution N 1 s XPS spectrum of the as-prepared electrode exhibits a peak of N = C and N-C bonds at 400.2 eV after being immersed into the electrolyte (Fig. 4d) [46]. When charged to 4.4 V (vs Li/Li⁺), a peak of -NH⁺ bonds at 402.0 eV arises, which is caused by the oxidation of -NH bonds [47,48]. The peak of -NH⁺ bonds disappears after discharging to 2.6 V (vs Li/Li⁺), which shows good reversibility of the p-type redox reaction. The peak of Cl 2p increases after charging and decreases after discharging, which is attributed to the insertion/deinsertion of ClO₄⁻ into/from the P-BQPZ, while the peak of Li 1 s shows the opposite trends (Fig. S15) [31]. Reversible appearance/disappearance of peaks at 1061 and 617 cm⁻¹ from ClO₄⁻ can also be observed by *ex situ* IR tests for cathode half-cell based on p-type reaction (Fig. S16) [49]. Therefore, the studies of *ex situ* XPS, IR and DFT calculations verify the proposed p-type reaction mechanism and also good reversibility.

Furthermore, we evaluated the actual electrochemical performance of the two types of all-organic batteries built by using two redox pairs of P-BQPZ. The anode material is lithium terephthalate (Li₂TP), which is a common organic anode material for LIBs and synthesized according to the previous route from literatures [50–52]. Two types of all-organic cells based on P-BQPZ cathode and Li₂TP anode were fabricated and both could operate well in the appropriate voltage ranges (Fig. 5, S18 and S19). The redox processes of the all-organic batteries based on n-type and p-type redox reactions of P-BQPZ are given in Fig. 5a. The all-organic battery based on n-type redox reaction of P-BQPZ gives high practical capacity over 200 mA h g⁻¹ at current of 500 mA g⁻¹ in the voltage of 0.1–2.7 V, which is stable during the following cycles

(Fig. 5b). The full cell based on p-type redox reaction of P-BQPZ displays a capacity of $\sim 100 \text{ mA h g}^{-1}$ at 50 mA g^{-1} between 0.1 and 3.4 V (Fig. 5c).

3. Conclusions

In this study, we demonstrated the design and synthesis of P-BQPZ with three charged states for two types of high-performance organic LIBs with different characteristics as needed. P-BQPZ is designed to combine maximum multiple redox-active groups (n-type and p-type moieties), minimum redox-inactive groups and stable polymer backbone. The cathode half-cell based on n-type redox reaction shows high retention and high capacity of $431.3 \text{ mA h g}^{-1}$ (at 50 mA g^{-1}) with a working potential of 2.4 V (vs Li/Li⁺), while the cathode half-cell based on p-type redox reaction displays high cycling stability and higher output potential over 3.0 V (vs Li/Li⁺) with a capacity of $176.6 \text{ mA h g}^{-1}$ (at 50 mA g^{-1}). Two types of all-organic batteries based on n-type and p-type reactions of P-BQPZ have been successfully fabricated and workable with one starting battery cathode material. These results demonstrated that P-BQPZ is an excellent organic cathode material with three charge states (two redox pairs) and different characteristics, and our proposed design strategy is promising to obtain better organic batteries materials with even higher performance to fully capitalize the potential of future organic batteries.

Declaration of competing interest

The authors declare no competing financial interest.

Declaration of Competing Interest

The authors declare that they have no known competing financial interests or personal relationships that could have appeared to influence the work reported in this paper.

CRedit authorship contribution statement

Yang Zhao: Conceptualization, Data curation, Formal analysis, Investigation, Validation, Writing – original draft, Writing – review & editing. **Manman Wu:** Formal analysis, Investigation, Validation, Writing – review & editing. **Hongtao Zhang:** Supervision, Writing – review & editing. **Zhen Ge:** Data curation, Formal analysis. **Chenxi Li:** Supervision, Writing – review & editing. **Yanfeng Ma:** Formal analysis, Supervision. **Yongsheng Chen:** Conceptualization, Data curation, Formal analysis, Funding acquisition, Project administration, Resources, Supervision, Validation, Writing – review & editing.

Acknowledgements

The authors gratefully acknowledge the financial support from National Natural Science Foundation of China (NSFC, 52090034), the National Natural Science Foundation of China (NSFC, 51633002) and Higher Education Discipline Innovation Project (B12015).

Supplementary materials

Supplementary material associated with this article can be found, in the online version, at doi:10.1016/j.ensm.2022.02.011.

References

- [1] J. Liang, X. Li, K.R. Adair, X. Sun, Metal halide superionic conductors for all-solid-state batteries, *Acc. Chem. Res.* 54 (2021) 1023–1033, doi:10.1021/acs.accounts.0c00762.
- [2] X. Zhang, A. Wang, X. Liu, J. Luo, Dendrites in lithium metal anodes: suppression, regulation, and elimination, *Acc. Chem. Res.* 52 (2019) 3223–3232, doi:10.1021/acs.accounts.9b00437.
- [3] Y. Chen, C. Wang, Designing high performance organic batteries, *Acc. Chem. Res.* 53 (2020) 2636–2647, doi:10.1021/acs.accounts.0c00465.

- [4] X. Xing, Y. Li, S. Wang, H. Liu, Z. Wu, S. Yu, J. Holoubek, H. Zhou, P. Liu, Graphite-based lithium-free 3D hybrid anodes for high energy density all-solid-state batteries, *ACS Energy Lett.* 6 (2021) 1831–1838, doi:10.1021/acsenenergylett.1c00627.
- [5] Y. Hu, W. Tang, Q. Yu, X. Wang, W. Liu, J. Hu, C. Fan, Novel insoluble organic cathodes for advanced organic K-Ion batteries, *Adv. Funct. Mater.* 30 (2020) 2000675, doi:10.1002/adfm.202000675.
- [6] G. Dai, Y. He, Z. Niu, P. He, C. Zhang, Y. Zhao, X. Zhang, H. Zhou, A dual-ion organic symmetric battery constructed from phenazine-based artificial bipolar molecules, *Angew. Chem. Int. Ed.* 58 (2019) 9902–9906, doi:10.1002/anie.201901040.
- [7] L. Xu, Z. Sun, Y. Zhu, Y. Han, M. Wu, Y. Ma, Y. Huang, H. Zhang, Y. Chen, A Li-rich layered-spinel cathode material for high capacity and high rate lithium-ion batteries fabricated via a gas-solid reaction, *Sci. China Mater.* 63 (2020) 2435–2442, doi:10.1007/s40843-020-1433-4.
- [8] R. Yang, W. Yao, B. Tang, F. Zhang, X. Lei, C.-S. Lee, Y. Tang, Development and challenges of electrode materials for rechargeable Mg batteries, *Energy Storage Mater.* 42 (2021) 687–704, doi:10.1016/j.ensm.2021.08.019.
- [9] X. Lei, Y. Zheng, F. Zhang, Y. Wang, Y. Tang, Highly stable magnesium-ion-based dual-ion batteries based on insoluble small-molecule organic anode material, *Energy Storage Mater.* 30 (2020) 34–41, doi:10.1016/j.ensm.2020.04.025.
- [10] L. Liu, N. Solin, O. Inganäs, Bio based batteries, *Adv. Energy Mater.* (2021) 2003713, doi:10.1002/aenm.202003713.
- [11] T.B. Schon, B.T. McAllister, P.-F. Li, D.S. Seferos, The rise of organic electrode materials for energy storage, *Chem. Soc. Rev.* 45 (2016) 6345–6404, doi:10.1039/C6CS00173D.
- [12] Y. Liang, Y. Yao, Positioning organic electrode materials in the battery landscape, *Joule* 2 (2018) 1690–1706, doi:10.1016/j.joule.2018.07.008.
- [13] A. Saal, T. Hagemann, U.S. Schubert, Polymers for battery applications—active materials, membranes, and binders, *Adv. Energy Mater.* (2020) 2001984, doi:10.1002/aenm.202001984.
- [14] Y. Lu, Q. Zhang, L. Li, Z. Niu, J. Chen, Design strategies toward enhancing the performance of organic electrode materials in metal-ion batteries, *Chem* 4 (2018) 2786–2813, doi:10.1016/j.chempr.2018.09.005.
- [15] S. Lee, G. Kwon, K. Ku, K. Yoon, S.K. Jung, H.D. Lim, K. Kang, Recent progress in organic electrodes for Li and Na rechargeable batteries, *Adv. Mater.* 30 (2018) 1704682, doi:10.1002/adma.201704682.
- [16] Z. Tie, Z. Niu, Design strategies for high-performance aqueous Zn/Organic batteries, *Angew. Chem. Int. Ed.* 59 (2020) 21293–21303, doi:10.1002/anie.202008960.
- [17] D. Xu, M. Liang, S. Qi, W. Sun, L.-P. Lv, F. Du, B. Wang, S. Chen, Y. Wang, Y. Yu, The progress and prospect of tunable organic molecules for organic lithium-ion batteries, *ACS Nano* 15 (2020) 47–80, doi:10.1021/acsnano.0c05896.
- [18] L. Zhang, H. Wang, X. Zhang, Y. Tang, A review of emerging dual-ion batteries: fundamentals and recent advances, *Adv. Funct. Mater.* 31 (2021) 2010958, doi:10.1002/adfm.202010958.
- [19] S. Chen, T. Jia, G. Zhou, C. Zhang, Q. Hou, Y. Wang, S. Luo, G. Shi, Y. Zeng, A cross-linked triphenylamine-based polymer cathode material with dual anion-cation reversible insertion for lithium ion battery, *J. Electrochem. Soc.* 166 (2019) A2543, doi:10.1149/2.0941912jes.
- [20] Y. Zhao, M. Wu, H. Chen, J. Zhu, J. Liu, Z. Ye, Y. Zhang, H. Zhang, Y. Ma, C. Li, Y. Chen, Balance cathode-active and anode-active groups in one conjugated polymer towards high-performance all-organic lithium-ion batteries, *Nano Energy* 86 (2021) 106055, doi:10.1016/j.nanoen.2021.106055.
- [21] M. Wu, Y. Zhao, B. Sun, Z. Sun, C. Li, Y. Han, L. Xu, Z. Ge, Y. Ren, M. Zhang, Q. Zhang, Y. Lu, W. Wang, Y. Ma, Y. Chen, A 2D covalent organic framework as a high-performance cathode material for lithium-ion batteries, *Nano Energy* 70 (2020) 104498, doi:10.1016/j.nanoen.2020.104498.
- [22] K. Sakaushi, E. Hosono, G. Nickerl, T. Gemming, H. Zhou, S. Kaskel, J. Eckert, Aromatic porous-honeycomb electrodes for a sodium-organic energy storage device, *Nat. Commun.* 4 (2013) 1485, doi:10.1038/ncomms2481.
- [23] F.A. Obrezkov, A.F. Shestakov, V.F. Traven, K.J. Stevenson, P.A. Troshin, An ultrafast charging polyphenylamine-based cathode material for high rate lithium, sodium and potassium batteries, *J. Mater. Chem. A* 7 (2019) 11430–11437, doi:10.1039/C8TA11572A.
- [24] J. Qin, Q. Lan, N. Liu, Y. Zhao, Z. Song, H. Zhan, A metal-free battery working at -80°C , *Energy Storage Mater.* 26 (2019) 585–592, doi:10.1016/j.ensm.2019.12.002.
- [25] K.S. Park, S.B. Schougaard, J.B. Goodenough, Conducting-polymer/iron-redox-couple composite cathodes for lithium secondary batteries, *Adv. Mater.* 19 (2007) 848–851, doi:10.1002/adma.200600369.
- [26] S. Lee, K. Lee, K. Ku, J. Hong, S.Y. Park, J.E. Kwon, K. Kang, Utilizing latent multi-redox activity of P-type organic cathode materials toward high energy density lithium-organic batteries, *Adv. Energy Mater.* 10 (2020) 2001635, doi:10.1002/aenm.202001635.
- [27] J. Wu, X. Rui, C. Wang, W.B. Pei, R. Lau, Q. Yan, Q. Zhang, Nanostructured conjugated ladder polymers for stable and fast lithium storage anodes with high-capacity, *Adv. Energy Mater.* 5 (2015) 1402189, doi:10.1002/aenm.201402189.
- [28] J. Xie, Z. Wang, Z.J. Xu, Q. Zhang, Toward a high-performance all-plastic full battery with a single organic polymer as both cathode and anode, *Adv. Energy Mater.* 8 (2018) 1703509, doi:10.1002/aenm.201703509.
- [29] Y. Xu, Y. Zhou, T. Li, S. Jiang, X. Qian, Q. Yue, Y. Kang, Multifunctional covalent organic frameworks for high capacity and dendrite-free lithium metal batteries, *Energy Storage Mater.* 25 (2019) 334–341, doi:10.1016/j.ensm.2019.10.005.
- [30] R. Shi, L. Liu, Y. Lu, C. Wang, Y. Li, L. Li, Z. Yan, J. Chen, Nitrogen-rich covalent organic frameworks with multiple carbonyls for high-performance sodium batteries, *Nat. Commun.* 11 (2020) 178, doi:10.1038/s41467-019-13739-5.
- [31] J. Bitenc, N. Lindahl, A. Vizintin, M.E. Abdelhamid, R. Dominko, P. Johansson, Concept and Electrochemical mechanism of an all anode-organic cathode battery, *Energy Storage Mater.* 24 (2019) 379–383, doi:10.1016/j.ensm.2019.07.033.

- [32] L. Gao, X. Ge, Z. Zuo, F. Wang, X. Liu, M. Lv, S. Shi, L. Xu, T. Liu, Q. Zhou, X. Ye, S. Xiao, High quality Pyrazinoquinoxaline-based Graphdiyne for efficient gradient storage of lithium ions, *Nano Lett.* 20 (2020) 7333–7341, doi:[10.1021/acs.nanolett.0c02728](https://doi.org/10.1021/acs.nanolett.0c02728).
- [33] H.P. Cong, X.C. Ren, P. Wang, S.H. Yu, Flexible graphene-polyaniline composite paper for high-performance supercapacitor, *Energy Environ. Sci.* 6 (2013) 1185–1191, doi:[10.1039/C2EE24203F](https://doi.org/10.1039/C2EE24203F).
- [34] L. Hou, Z. Hu, H. Wu, X. Wang, Y. Xie, S. Li, F. Ma, C. Zhu, 2-Amino-3-chloro-1,4-naphthoquinone-covalent modification of graphene nanosheets for efficient electrochemical energy storage, *Dalton Trans.* 48 (2019) 9234–9242, doi:[10.1039/C9DT00895K](https://doi.org/10.1039/C9DT00895K).
- [35] D. Sui, L. Xu, H. Zhang, Z. Sun, B. Kan, Y. Ma, Y. Chen, A 3D Cross-linked graphene-based honeycomb carbon composite with excellent confinement effect of organic cathode material for lithium-ion batteries, *Carbon* 157 (2020) 656–662, doi:[10.1016/j.carbon.2019.10.106](https://doi.org/10.1016/j.carbon.2019.10.106).
- [36] S.R. Sivakumar, R. Saraswathi, Application of Poly(o-phenylenediamine) in rechargeable cells, *J. Appl. Electrochem.* 34 (2004) 1147–1152, doi:[10.1007/s10800-004-3302-8](https://doi.org/10.1007/s10800-004-3302-8).
- [37] C. Han, J. Tong, X. Tang, D. Zhou, H. Duan, B. Li, G. Wang, Boost anion storage capacity using conductive polymer as a Pseudocapative cathode for high-energy and flexible lithium ion capacitors, *ACS Appl. Mater. Interfaces* 12 (2020) 10479–10489, doi:[10.1021/acsami.9b22081](https://doi.org/10.1021/acsami.9b22081).
- [38] C. Zhao, Z. Chen, W. Wang, P. Xiong, B. Li, M. Li, J. Yang, Y. Xu, Situ Electropolymerization enables ultrafast long cycle life and high-voltage organic cathodes for lithium batteries, *Angew. Chem. Int. Ed.* 59 (2020) 11992–11998, doi:[10.1002/anie.202000566](https://doi.org/10.1002/anie.202000566).
- [39] H. Tang, L. You, J. Liu, S. Wang, P. Wang, C. Feng, Z. Guo, Integrated Polypyrrole@Sulfur@Graphene Aerogel 3D architecture via advanced vapor polymerization for high-performance lithium–sulfur batteries, *ACS Appl. Mater. Interfaces* 11 (2019) 18448–18455, doi:[10.1021/acsami.9b04167](https://doi.org/10.1021/acsami.9b04167).
- [40] T. Sun, Z.J. Li, H.G. Wang, D. Bao, F.L. Meng, X.B. Zhang, A biodegradable Polydopamine-derived electrode material for high-capacity and long-life lithium-ion and sodium-ion batteries, *Angew. Chem. Int. Ed.* 55 (2016) 10662–10666, doi:[10.1002/anie.201604519](https://doi.org/10.1002/anie.201604519).
- [41] T. Nokami, T. Matsuo, Y. Inatomi, N. Hojo, T. Tsukagoshi, H. Yoshizawa, A. Shimizu, H. Kuramoto, K. Komae, H. Tsuyama, J.I. Yoshida, Polymer-bound Pyrene-4,5,9,10-tetraone for fast-charge and -discharge lithium-ion batteries with high capacity, *J. Am. Chem. Soc.* 134 (2012) 19694–19700, doi:[10.1021/ja306663g](https://doi.org/10.1021/ja306663g).
- [42] T. Ma, Q. Zhao, J. Wang, Z. Pan, J. Chen, A sulfur heterocyclic quinone cathode and a multifunctional binder for a high-performance rechargeable lithium-ion battery, *Angew. Chem. Int. Ed.* 55 (2016) 6428–6432, doi:[10.1002/anie.201601119](https://doi.org/10.1002/anie.201601119).
- [43] A. Vizintin, J. Bitenc, A. Kopač. Lautar, K. Pirnat, J. Grdadolnik, J. Stare, A. Randon-Vitanova, R. Dominko, Probing electrochemical reactions in organic cathode materials via in operando infrared spectroscopy, *Nat. Commun.* 9 (2018) 661, doi:[10.1038/s41467-018-03114-1](https://doi.org/10.1038/s41467-018-03114-1).
- [44] J. Hong, M. Lee, B. Lee, D.H. Seo, C.B. Park, K. Kang, Biologically inspired pteridine redox centres for rechargeable batteries, *Nat. Commun.* 5 (2014) 5335, doi:[10.1038/ncomms6335](https://doi.org/10.1038/ncomms6335).
- [45] L. Huang, Y. Chen, Y. Liu, T. Wu, H. Li, J. Ye, G. Dai, X. Zhang, Y. Zhao, π -extended Dihydrophenazine-based polymeric cathode material for high-performance organic batteries, *ACS Sustain. Chem. Eng.* 8 (2020) 17868–17875, doi:[10.1021/acssuschemeng.0c07314](https://doi.org/10.1021/acssuschemeng.0c07314).
- [46] X. Li, H. Wang, Z. Chen, H.S. Xu, W. Yu, C. Liu, X. Wang, K. Zhang, K. Xie, K.P. Loh, Covalent-organic-framework-based Li–CO₂ batteries, *Adv. Mater.* (2019) 1905879, doi:[10.1002/adma.201905879](https://doi.org/10.1002/adma.201905879).
- [47] Z. Yang, T. Wang, H. Chen, X. Suo, P. Halstenberg, H. Lyu, W. Jiang, S.M. Mahurin, I. Popovs, S. Dai, Surpassing the organic cathode performance for lithium-ion batteries with robust fluorinated covalent quinazoline networks, *ACS Energy Lett.* 6 (2020) 41–51, doi:[10.1021/acseenergylett.0c01750](https://doi.org/10.1021/acseenergylett.0c01750).
- [48] Y. Zhao, Y. Wang, Z. Zhao, J. Zhao, T. Xin, N. Wang, J. Liu, Achieving high capacity and long life of aqueous rechargeable zinc battery by using Nanoporous-carbon-supported Poly(1,5-naphthalenediamine) Nanorods as cathode, *Energy Storage Mater.* 28 (2020) 64–72, doi:[10.1016/j.ensm.2020.03.001](https://doi.org/10.1016/j.ensm.2020.03.001).
- [49] A. Jouhara, E. Quarez, F. Dolhem, M. Armand, N. Dupré, P. Poizot, Tuning the chemistry of organonitrogen compounds for promoting all-organic anionic rechargeable batteries, *Angew. Chem. Int. Ed.* 58 (2019) 15680, doi:[10.1002/anie.201908475](https://doi.org/10.1002/anie.201908475).
- [50] H.H. Lee, Y. Park, K.H. Shin, K.T. Lee, S.Y. Hong, Abnormal excess capacity of conjugated Dicarboxylates in lithium-ion batteries, *ACS Appl. Mater. Interfaces* 6 (2014) 19118–19126, doi:[10.1021/am505090p](https://doi.org/10.1021/am505090p).
- [51] M. Armand, S. Grugeon, H. Vezin, S. Laruelle, P. Ribiere, P. Poizot, J.M. Tarascon, Conjugated Dicarboxylate anodes for Li-ion batteries, *Nat. Mater.* 8 (2009) 120–125, doi:[10.1038/nmat2372](https://doi.org/10.1038/nmat2372).
- [52] Q. Pan, Y. Zheng, Z. Tong, L. Shi, Y. Tang, Novel lamellar Tetrapotassium Pyromellitic organic for robust high-capacity potassium storage, *Angew. Chem. Int. Ed.* 60 (2021) 11835–11840, doi:[10.1002/anie.202103052](https://doi.org/10.1002/anie.202103052).